Available online www.jsaer.com

***Journal of Scientific and Engineering Research*, 2020, 7(10):90-100**

Research Article

ISSN: 2394-2630
CODEN(USA): JSERBR

Development and Characterization of Mineral Microfiltration Membranes Deposited on Flat Ceramic Supports Based on Natural Cameroonian Clay

Fabrice Wandji Ndiapa*[1], Joseph Marie Sieliechi[1], Martin Benoit Ngassoum[1], Marc Cretin[2], Sophie Cerneaux[2], Didier Cot[2], Nathalie Masquelez[2]

[1]Department of Applied Chemistry, University of Ngaoundéré, P.O. Box 455, Ngaoundéré, Cameroon
[2]Institut Européen des Membranes, IEM - UMR 5635, ENSCM, CNRS, Univ Montpellier, Case courrier 047, 34095 Montpellier Cedex 5, Montpellier, France
*Corresponding author, email: fabricendiapa@yahoo.fr

Abstract The elaboration and characterization of flat porous ceramic support and microfiltration membrane, using clay from Yagoua region (Far North of Cameroon) were reported. The selection of raw materials (clay and rice husk) was primarily based on their low cost and they are locally produced. The clay powder was characterized by Energy Dispersive X-Ray analysis, X-Ray diffraction, Thermal analysis. The consolidated ceramic substrates were characterized by Hg intrusion, mechanical resistance. A ceramic support, sintered at 1100 °C, within an average pore size of 6.21 µm, a porosity of 43.73 % and compression strength of 10.42 MPa, was prepared. The microfiltration membrane layer sintered at 900 °C has an average pore size value of 0.33 µm and porosity of 35.36 %. This membrane reduced by 99.8 % the turbidity of an effluent containing suspended particles.

Keywords clay, rice husk, ceramic support, microfiltration membrane, Slip casting

1. Introduction

Due to the extremely low impact on the environment (with new requirements concerning to materials) and reduced operating costs (preparation procedures), membrane separation processes extend more every day in industrial uses. The use of inorganic membranes with respect of organic membranes has rapidly increased during the last two decades due to their potential application in a wide range of industrial processes such as water and effluent treatments [1, 2], drink clarification [3, 4].

Ceramic membranes have many known advantages such as high thermal and chemical stability, pressure resistance, long lifetime, and catalytic properties from their intrinsic nature [5, 6]. Several materials are usually employed for the preparation of ceramics membranes, such as alumina, zirconia and titania. The development of ceramic membranes based on natural materials and fly ashes was investigated by several authors, mostly attending to the economical advantages. New composite ceramic microfiltration and ultrafiltration membranes have been produced recently from abundant natural materials like clay [7] and phosphate [8]. Majouli [9] described the elaboration of new tubular ceramic membrane from local Moroccan perlite.

In this work, novel microfiltration (MF) ceramic membranes, made of thinner active layer supported on a porous support, have been prepared. The different substrates (support and ceramic membrane) are prepared controlling the particle size, the paste formulation, the deposition time and the thermal treatment. The microfiltration ceramic membranes were characterized for evaluating their morphology, porosity, mechanical properties.

2. Materials and Methods

2.1. Raw materials

Powders of natural clay and rice husk were used as starting materials in the present work. These raw materials were obtained from Yagoua region (Far North of Cameroon). Rice husk powder was used as a pore former.

2.2. Ceramic supports elaboration

Porous flat membrane supports were fabricated from natural clay, rice husk and water. The powders were then ground and sieved through a 100 µm sieve. Ceramic pastes compositions for the synthesis of flat ceramic supports were 70-30, as clay-rice husk ratio, sintered respectively at 900 °C, 1000 °C, 1100 °C and 1200 °C. Clay powders were accurately weighed according to the composition and mixed with the determined volume of Millipore water to make the paste for calendaring. After that, the paste was left for 24 h under a high humidity to improve its rheological property. After which, the membrane was dried at 100 °C for 24 h. Afterwards, the supports were sintered at different temperatures ranging from 900 °C to 1200 °C for 2 h, with a heating rate of about 2 °C/min from 25 °C to final temperature Tf (°C).

2.3. Membrane Elaboration

These membrane configurations consist of two layers: a porous support, an interlayer layer. The interlayer was prepared from the same clay powder used to make ceramic support. Deposition of the intermediate layer was performed with a colloidal process (slip-casting process). This involves the preparation of a stable suspension, using clay, polyvinyl alcohol (PVA) used as a binder and water. Table 1 presents different formulations of barbotine for the synthesis of the microfiltration membrane. The suspension was then deposited on the support using the slip casting method (different depositions time were 2, 4, 6 min). The used support, sintered at 1100 °C, has an average pore size (APS) of 6.21 µm and 43.73 % porosity. The system was dried vertically for about 24 h at room temperature and it was subsequently sintered at 900 °C for 2 h with a heating rate of about 5 °C/min.

Table 1: Different formulations of barbotine suspensions (%Weight)

Barbotines	Clay powder (%)	Polyvinyl alcohol (PVA) (12 % in weight) (%)	Distilled water (%)
BA1	4	20	76
BA2	4	30	66
BA3	4	40	56
BA4	7	20	73
BA5	7	30	63
BA6	7	40	53
BA7	10	20	70
BA8	10	30	60
BA9	10	40	50

*BA : Barbotine

Figure 1 presents the steps of the elaboration of the microfiltration mineral membranes.

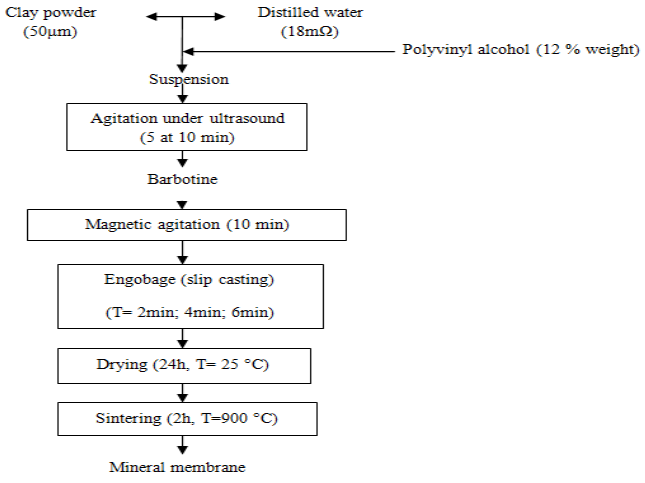

Figure 1: Schematic representation of the ceramic membrane preparation

The firing temperature, fixed at 900 °C, is reached following the thermal program. A temperature plate at 500 °C for 1 h is necessary in order to completely eliminate the PVA, which is in great quantities in the slip.

2.4. Characterizations techniques

The elementary chemical composition of clay powder was achieved using a Hitachi S4500 microscope with an acceleration voltage ranging from 0.5 kV to 30 kV. This microscope was coupled to an Energy Dispersive X-ray detector.

X-ray diffraction technique was used to identify the phase formations after substrate sintering. The structure was determined using a Philips X'Pert X-ray diffractometer operating with Cu Kα radiation source (λ = 1.54056 Å) and a Secondary beam crystal monochromator. The samples were scanned at diffraction angle 2θ from 5 to 50.

Thermogravimetric (TGA) analysis and Differential Scanning Calorimetry (DSC) analysis were performed with the TA Instruments SDT 2960 Simultaneous DSC-TGA. These two analyses were carried out under air atmosphere, with a heating rate of 10 °C/min, from 0 °C to 1000 °C.

The porosity and average pore diameter of the sintered substrates were determined using Mercury Intrusion Porosimetry (MIP) with an Autopore IV 9500 V1.06 (Micromeritics Instrument Corporation) porosimeter, working range from low pressure from 0 to 414 MPa corresponding to a pore sizes from 360 to 3.6 µm.

A Hitashi S4800 Scanning Electron Microscope (SEM) with the acceleration voltage varying from 0.1 kV to 30 kV was used to study the powder morphology as well as the microstructure formed in the sintered membrane.

The fracture strength module of the sintered materials was obtained by using the three-point bending method according to ASTM C674-88 using "LLOYD LRX" instruments. The specimens used for the measurement of the flexural strength are rectangular in shape (60 mm length, 21 mm width and 3 mm thickness).

The chemical corrosion resistance, of the fabricated ceramic membranes sintered at 900 °C, was evaluated by the mass loss after being immersed into HNO_3 (pH=1.1) and NaOH solutions (pH=12.38) at a room temperature for 7 days.

Microfiltration tests were performed using a home-made pilot plant (Fig. 2) at a temperature of 25 °C and transmembrane pressure (TMP) range between 1 and 2 bars.

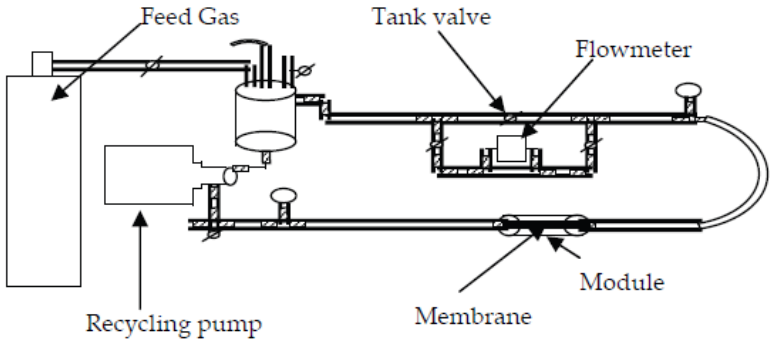

Figure 2: Flow schema of experimental apparatus

The flow rate was fixed at 2.5 $m.s^{-1}$. Before the tests, the membrane was conditioned by immersion in pure deionised water for a minimum of 24 h. The working pressure was obtained using a nitrogen gas source.

3. Results and Discussion

3.1. Raw Materials Analysis

3.1.1. Elementary Chemical Composition

The chemical analysis of the clay powder is given in Table 2. Results corresponded to an average of three measurements performed in various areas of the material surface.

Table 2: Chemical composition of the clay powder

Element	C	O	Na	Mg	Al	Si	S	K	Ca	Ti	Fe	Total
Mean (wt.%)	10.62	59.20	0.24	0.21	8.50	16.40	0.21	1.07	0.29	0.43	2.85	-
Standard deviation	0.67	1.15	0.08	0.01	0.18	0.75	0.04	0.38	0.11	0.06	0.43	-

The clay material studied is predominantly characterized by respective mass contents of silicon and aluminum of 16.4 % and 8.5 %. These elements are present in the clay in the form of Al_2O_3, and SiO_2 oxides. The silica and alumina present in the clay matrix form the skeletal structure of the ceramic substrates after calcination. The minor chemical elements, Na, Mg, Ca, K, Ti, form the corresponding oxides Na_2O, CaO, MgO, K_2O, TiO_2.

3.1.2. X – ray Diffraction analysis (XRD)

The XRD pattern of the clay used as raw material for the formulation of the ceramic filters are represented in Figure 3.

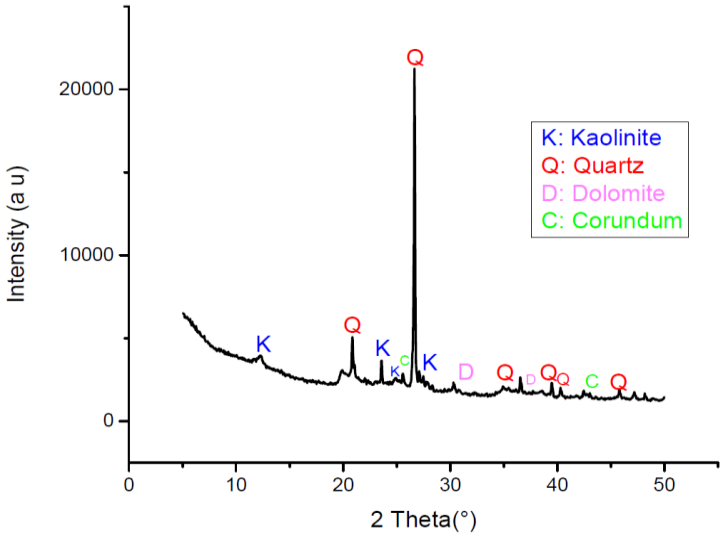

Figure 3: XRD pattern of Yagoua clay (K = kaolinite, Q = Quartz, D = Dolomite, C = Corundum)

The different crystal phases mainly identified in the clay powder according to JCPDS data base file are constituted by kaolinite ($Al_2Si_2O_5$ $(OH)_4$), quartz (SiO_2), dolomite $CaMg(CO_3)_2$ and corundum (Al_2O_3).

3.1.3. Thermal analysis: Thermogravimetric analysis (TGA) – Differential scanning calorimetry (DSC)

The curves for TGA/DSC analysis of this clay were shown in Figure 4.

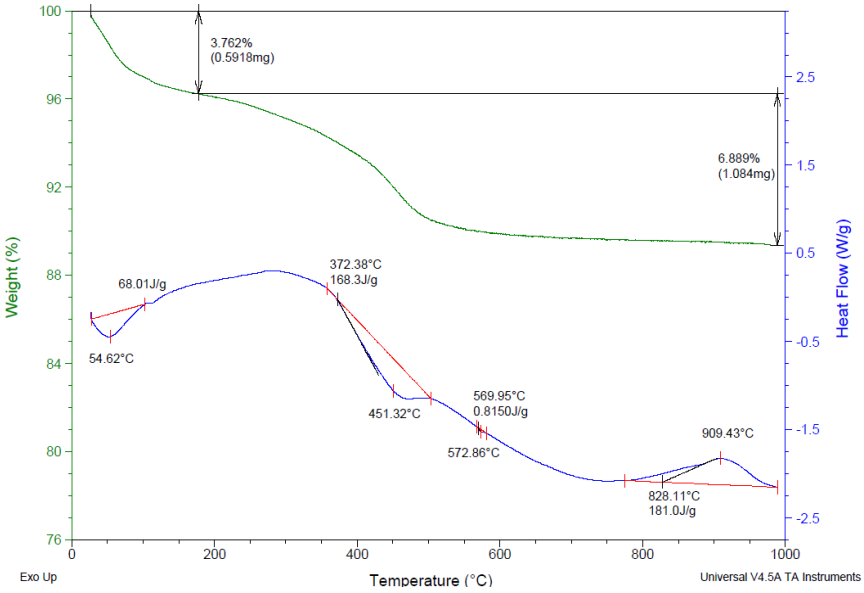

Figure 4: TGA-DSC curves of the crude clay powder

The TGA curve shows two important mass losses:

- The first loss of 3.8 % extending up to 160 °C corresponds to the elimination of water adsorbed on the surface and present between the lamellar structures of the clay.

- The second loss of 6.9 % occurs at about 500 °C and corresponds to the decomposition of hydroxyl groups and carbonates [10].

The DSC curve shows three important peaks:

- A first endothermic peak at 54.6 °C is due to the departure of the surface water (dehydration);
- A second endothermic peak, large and asymmetric at 451.3 °C, corresponds to decomposition (dehydroxylation) of mixed carbonates of magnesium and calcium (dolomite) [11]. During this step, the transformation of kaolinite into metakaolinite occurs (1) [12-15].

$2SiO_2 .Al_2O_3 .2H_2O$. (Kaolinite) $\longrightarrow$ $2SiO_2.Al_2O_3$ (metakaolinite) + $2H_2O$ (1)

- The exothermic peak at 909.43 °C with no weight loss corresponds to the structural reorganization of the minerals with the formation of a spinel phase from metakaolinite (corresponding to mullite formation) [26]; [13-15]). The most common descriptions are summarized in reactions (2) and (3):

$2SiO_2.Al_2O_3$ (metakaolinite) $\longrightarrow$ $SiAl_2O_4$ (spinel) + SiO_2 (amorphous) (2)

$2SiO_2.Al_2O_3$ (metakaolinite) $\longrightarrow$ $2Al_2O_3$ (γ-alumina) + 2 SiO_2 (amorphous) (3)

3.2. Ceramic support and membrane characterizations

3.2.1. Mercury intrusion porosimetry

The total porosity and average pore size have been determined by mercury intrusion porosimetry for supports sintered at different temperatures for 2 h. Structural characteristics of the final membrane supports, prepared from Yagoua clay and rice husk + water, are summarized in Table 3.

Table 3: Properties of ceramic supports prepared from Yagoua clay and rice husk

Samples	Sintering temperature (°C)	Total porosity (±0.01%)	Average pore size (APS) (µm)	Tensile strength (MPa)
A1	900	52.59	1.55	4.06
A2	1000	50.46	2.66	4.95
A3	1100	43.73	6.21	10.42
A4	1200	28.75	7.72	15.65

The open porosity and the average pore size (APS) of the porous membrane supports sintered at different temperatures for 1 h are illustrated in Figure 5.

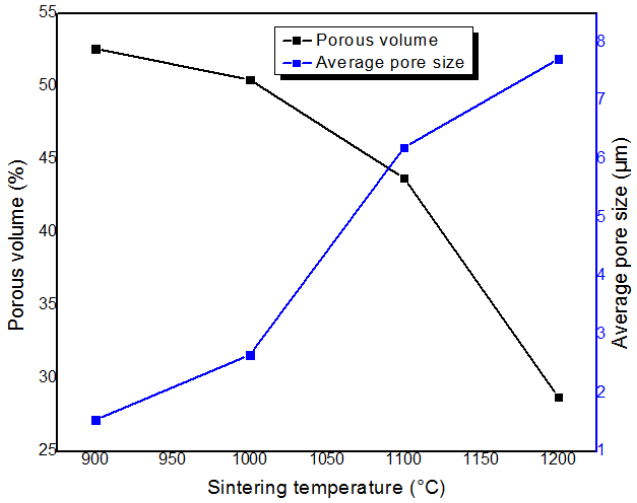

Figure 5: Porous volume (%) and average pore size vs sintering temperature for ceramic supports

As would be expected, this figure shows, generally that there is an increase in average pore size and a decrease in total porosity in samples, when the sintering temperature is increased. Pore size measurements have confirmed the dependence of the pore diameter on the sintering temperature. In fact, the values estimated from mercury porosimetry are 1.55 µm, 2.66 µm, 6.21 µm and 7.72 µm for 900 °C, 1000 °C, 1100 °C and 1200 °C respectively. It is clear that higher the sintering temperature larger the pore diameter of the support. This result is in agreement with other works [17]. The increase in average pore size is also confirmed by typical micrographs illustrated in Figure 7.

3.2.2. Compressive strength

The effect of sintering temperature on the mechanical properties of the membrane supports was also investigated. The mechanical resistance tests have been carried out by the three points bending method (Lloyd Instrument, France) to control the resistance of the support tube fired at different temperatures. Fig. 6 shows the changes in the compressive mechanical strength of the porous ceramics supports sintered at different temperatures (from 900 °C to 1200 °C).

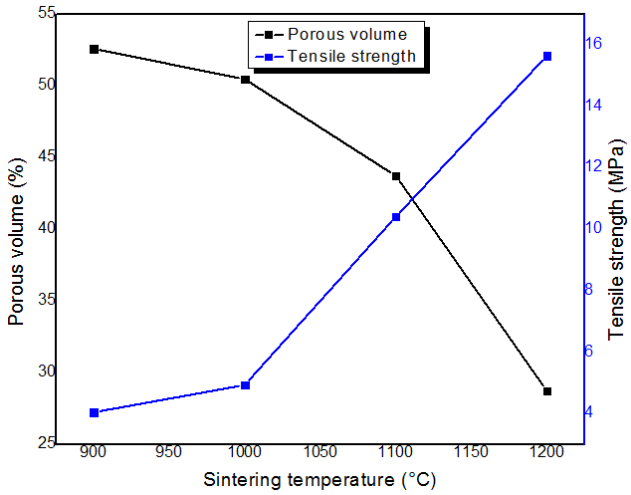

Figure 6: Flexural strength vs sintering temperature of ceramic supports using three bending point method test

The compressive strengths of specimens progressively increase with the increase in sintering temperature. The increase of the sintering temperature has been accompanied by a densification phenomenon and consequently an increase in the flexural strength (from 4.06 MPa at 900 °C to 15.65 MPa at 1200 °C). Usually, densification and grain size are the dominant factors controlling the mechanical strength, since most of the total pores were intergranular. The substantial increase in strengths of samples corresponded to a parallel increase in density, which means a decrease in porosity ratio. The material sintered at 1100 °C (A3) has reached a flexural strength of 10.42 MPa, which represents a good support mechanical resistance, compared with clay or phosphate tubular supports [12, 17-19].

3.2.3. Scanning Electron Microscopy (SEM)

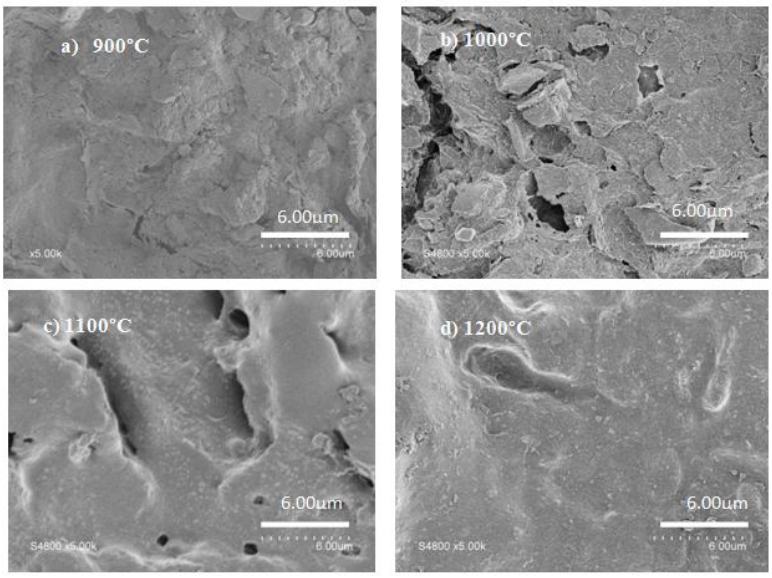

Figure 7: SEM micrographs of ceramic supports (a, b, c, d) at different sintering temperatures (900 °C, 1000 °C, 1100 °C, 1200 °C)

Figure 7 shows SEM images of the surface support sintered at different temperatures. They thus describe the evolution of the microstructure of the supports with the increase in the sintering temperature (from 900 °C to

1200 °C). The progressive reduction of the porosity can be observed with the increase of the sintering temperature.

Consolidation between the grains by the effect of heat begins at 900 °C. At the turn of 1000 °C, the grains are sufficiently close and the internal reorganization of each of them is well established thus forming a surface of high roughness. The presence of the intergranular contacts ensures the cohesion of the ceramic. At 1100 °C, the densification is produced by welding and magnification of the grains. There is a more or less irregular growth of particles. A smoothing of the grains at the surface leads to a low roughness, which may allow the deposition of a layer. At 1200 °C, a gradual disappearance of the small grains in favor of the bigger ones is the beginning of the vitrification. At 1100 °C, the support surface has been homogeneous and has not presented any cracks. A smooth inner surface has been also observed, allowing the effective deposit of an active fine layer membrane. These results are in agreement with those observed in the literature [20, 21].

3.3. Intermediate layer characterization

3.3.1. Determination of the porosity

Total porous volume and pore size distribution are measured by mercury porosimetry. The pore diameters measured were centered near 0.33 µm and the total porous volume were 35.36 % for the deposited microfiltration layer. This average pore size (APS) indicates that this kind of membranes can be utilized in the Microfiltration range (MF). This APS value is considerably lower than those obtained for other typical ceramic MF membranes (about 0.5 µm) reported in previous works [22, 23].

3.3.1.1. Surface morphology and cross-section

The thickness of the active layer increased with casting time respectively from 3.01 µm for 2 min, to 15 µm for 6 min and to 18.7 µm for 6 min casting time (Figure 8).

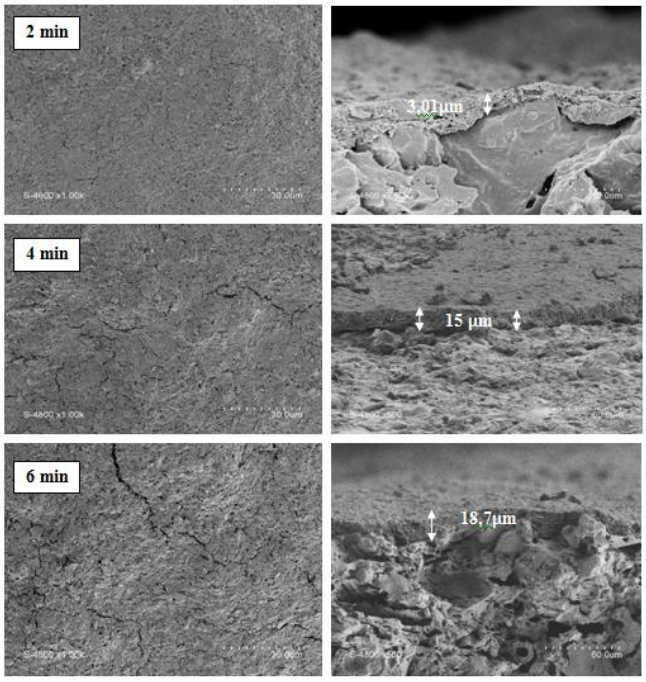

Figure 8: SEM micrographs for ceramic microfiltration membrane obtained with different casting times

When analyzing the surface texture of different samples, it can be concluded that the sample obtained with 2 min casting time de not contain defects (cracks and pinholes) at the opposite of all other samples.

3.3.2. Chemical corrosion

The chemical corrosion resistance, of the fabricated membranes sintered at 900 °C, was evaluated by the mass loss after being immersed into HNO_3 (pH= 1) and NaOH solutions (pH=13) at 80 °C for 7 days. The weight loss due to the corrosion of acids and alkali is shown in figure 9. During 12 days at atmospheric conditions the weight loss does not exceed 0.3 weight % in acid medium. However, in basic medium, the weight loss reaches 0.95 weight %.

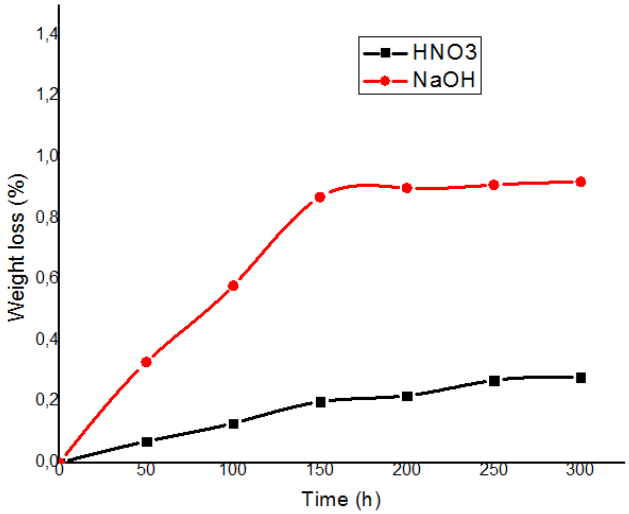

Figure 9: Weight loss of support in acidic medium (HNO_3 solution at pH = 1) and basic medium (NaOH solution at pH= 13)

It can be seen that the membrane shows a better alkali corrosion resistance, since its mass loss is much lower than those of membranes after acid corrosion. This can be explained by the high alkali content of the considered ceramics [24].

3.3.3. Filtration of effluent containing suspended particles

The permeate flux as function to transmembrane pressure is presented in Figure 10. It was found that the curve of permeate flux as function of applied pressure is linear and its slope that corresponds to the value of permeability is about 819.7 L/h m^2 bar.

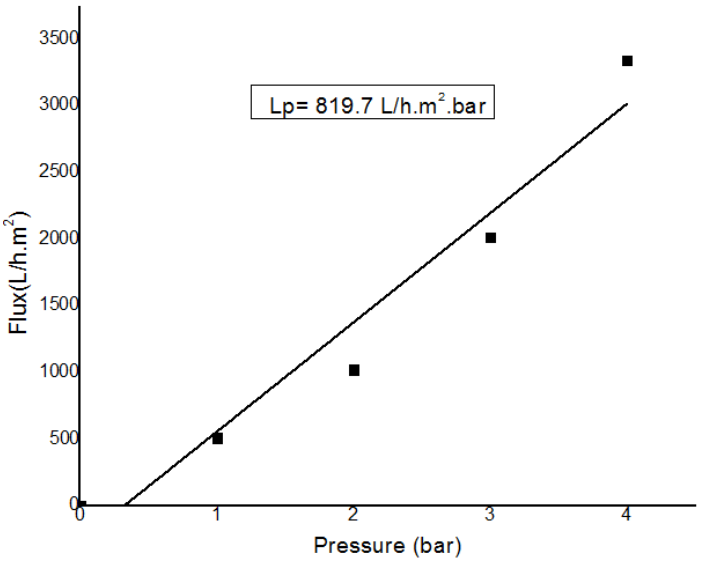

Figure 10: Water flux versus transmembrane pressure

A ceramic microfiltration membrane was employed to treat effluent containing suspended matter at a pressure between 1 and 2 bar during 120 min of filtration at room temperature. Table 4 reports the characteristics of the effluent before and after microfiltration treatment.

Table 4: Characteristics of the effluent before and after filtration

Parameters of Effluent	Before treatment	After treatment
pH	5.61	5.58
Conductivity (µS/cm)	230.87	230.85
Turbidity (NTU)	250	2.75

The Figure 11 shows the evolution of the flux of the effluent at different pressure (1 and 2 bar) as a function of filtration time. The results show that permeate flux for the effluent gradually decrease with filtration time due to the accumulation of suspended particles conducting to formation of a cake on the surface of the membrane. It is observed that permeate flux approximately dropped by 86 % for the effluent 819.7–115 L/h m^2 at 2 bar after 2 h of filtration. The percentage of reduction of turbidity for this effluent is 98.8 %.

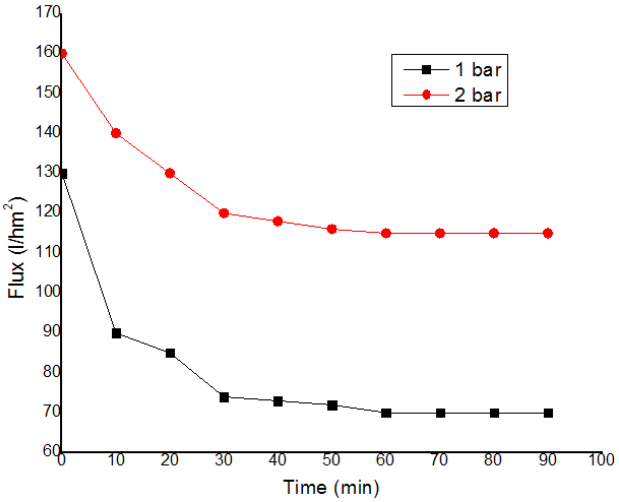

Figure 11: Evolution of permeate flux of effluent with filtration time for 1 bar and 2 bar

4. Conclusion

In this work, a comprehensive study on the fabrication and characterization of flat ceramic membranes from aluminosilicates was performed. Ceramic supports have been obtained by rolling process using clay and rice husk as starting materials.

The prepared supports sintered at 1100 °C for 2h offer a better mechanical strength (10.4 MPa), chemical stability (<5 % weight loss) good porosity (43.7 %), better average pore size (6.2 µm). It has also been concluded that the membrane supports sintered at 1100 °C is the optimum supports allowed for depositing the membrane layers.

Moreover, microfiltration ceramic membranes were prepared by slip casting method. The optimized composition of the slip was determined: 20 % PVA, 76 % water and 4 % clay powder, with a slip casting time of 2 min. The flat ceramic membranes showed the following structural characteristics: porosity of 35.36 %, average pore size (APS) of about 0.33 µm, active layer thickness around 3.01 µm, support thickness, 3 mm. The turbidity of an effluent containing suspended particles was reduced of 99.8 %. This result may allow the novel membrane to be used in water treatment in the microfiltration range.

Acknowledgments

The authors gratefully acknowledge the partial financial support received from the "AUF" (Agence Universitaire de la Francophonie), "BACGL" (Bureau Afrique Centrale et Grands Lacs) and thank Prof. Philippe Miele Director General of Membrane European Institute ("IEM") for equipment delivering facilities (Hg-Porosimeter, XRD, BET, TGA-DSC, FTIR, SEM,…) and his continuous encouraging on the subject.

References

[1]. Xu, L., Li. W., Lu, S., Wang, Z., Zhu, Q., Ling, Y., Treating dyeing waste water by ceramic membrane in cross flow microfiltration, Desalination, 149, 2002, 199–203.

[2]. Ebrahimi, M., Shams Ashaghi, K., Engel, L., Willershausen, D., Mund, P., Bolduan, P., Czermak, P., Characterization and application of different ceramic membranes for the oil-field produced water treatment, Desalination, 245, 2009, 533–540.

[3]. Nandi, B. K., Das, B., Uppaluri, R., Purkait, M. K., Microfiltration of mosambi Juice using low cost ceramic membrane, J. Food Eng, 95, 2009, 597–605.

[4]. Vaillant, F., Millan, A., Dornier, M., Decloux, M., Reynes, M., Strategy for Economical optimization of the clarification of pulpy fruit juices using cross flow microfiltration, J. Food Eng, 48, 2001, 83–90.
[5]. Burggraaf, A. J., Cot, L., Fundamentals of Inorganic Membrane Science and Technology, Elsevier Science, Amsterdam, The Netherlands, 1996.
[6]. Li, K., Ceramic Membranes for Separation and Reaction, John Wiley and Sons Ltd, West Sussex, England, 2007.
[7]. Elomari, H., Achiou, B., Ouammou, M., Albizane, A., Bennazha, J., Alami Younssi, S., Elamrani, I.,. Elaboration and characterization of flat membrane supports from Moroccan clays. Application for the treatment of wastewater. Desalin. Water Treat, 2015, 1–9.
[8]. Khemakhem, M., Khemakhem, S., Ayedi, S., Ben Amar, R., Study of ceramic ultrafiltration membrane support based on phosphate industry sub product: application for the cuttlefish conditioning effluents treatment. Ceram. Int. 37, 2011, 3617–3625.
[9]. Majouli, A., Tahiri, S., Alami Younssi, S., Loukili, H., Albizane, A.,. Elaboration of new tubular ceramic membrane from local Moroccan perlite for microfiltration process: application to treatment of industrial wastewaters. Ceram. Int. 38, 2012, 4295.
[10]. Qabaqous, O., Tijani, N., Naciri Bennani1, M., El Krouk, A., Elaboration et caractérisation des supports plans à base d'argile (Rhassoul) pour membranes minérales. *Mater. Environ. Sci. 5 (S1)*, 2014, *2244-2249.*
[11]. Abdelaziz, B, Thèse de Doctorat, Université cadi ayyad, Faculté des sciences Semlalia Marrakech (juillet 2005).
[12]. Benazzouz, B. K. and Zaoui, A., "Thermal behaviour and superheating temperature of Kaolinite from molecular dynamics," Applied Clay Science vol. 58, 2012, pp. 44-51.
[13]. Ilić, B. R., Mitrović, A. A., and Miličić, L. R., "Thermal treatment of kaolin clay to obtain metakaolin," Hem.Ind, vol. 64, 2010, pp. 351-356.
[14]. Ptáček, P., Kubátová, D., Havlica, J., Brandštetr, J., Šoukal, F., and Opravil, T., "The nonisothermal kinetic analysis of the thermal decomposition of kaolinite by thermogravimetric analysis," Powder technology, vol. 204, 2010, pp. 222-227.
[15]. Traoré, K., Blanchart, P., Jernot, J.-P., and Gomin, M., "Caractérisation physicochimique et mécanique de matériaux céramiques obtenus à partir d'une argile kaolinitique du Burkina Faso," C. R. Chimie, vol. 10, 2007, pp. 511-519.
[16]. Gridi-bennadji, F, "Matériaux de mullite à microstructure organisée composes d'assemblages muscovite-kaolinite," France, Université de Limoges. 2007.
[17]. Khemakhem, S., Ben Amar, R., Ben Hassen, R., Larbot, A., Ben Salah, A., Cot, L., Fabrication of mineral supports of membranes for microfiltration/ultrafiltration from tunisian clay, Ann. Chim. Sci. Mater., 31, 2006, 169–181.
[18]. Belibi, P., Nguemtchouin, M. M. G., Rivallin, M., Nsami, J. N., Sieliechi, J., Cerneaux, S., Ngassoum, M. B., Cretin, M., Microfiltration ceramic membranes from local Cameroonian clay applicable to water treatment, Ceram. Int., 41, 2015, 2752–2759.
[19]. Saffaj, N., Persin, M., Younsi, S. A., Albizane, A., Cretin, M., Larbot, A., Elaboration and characterization of microfiltration and ultrafiltration membranes deposited on raw support prepared from natural Moroccan clay: application to filtration of solution containing dyes and salts, Appl. Clay. Sci., 31, 2006, 110–119.
[20]. Bouazizi, A., Saja, S., Achiou, B., Ouammou, M., Calvo, J. I., Aaddane, A., Alami Younssi, S.,. Elaboration and characterization of a new flat ceramic MF membrane made from natural Moroccan bentonite. Application to treatment of industrial wastewater. Journal of Applied Clay Science 132–133, 2016, 33–40.
[21]. Lahsini, A., Bentama, J., Addaou, A., Rafiq, M., Caractérisation physico-chimique et étude du frittage d'une argile destinée à l'élaboration de membranes de filtration tangentielle. J. *Chim. Phys,* **95,** 1998, 1001-1019.

[22]. Harabi, A., Bouzerara, F., Condom, S., Preparation and characterization of tubular membrane supports using centrifugal casting, Desalin. Water. Treat. 6, 2009, 222–226.
[23]. Bouzerara, F., Harabi, A., Condom, S., Porous ceramic membranes prepared from kaolin, Desalin. Water. Treat, 12, 2009, 415–419.
[24]. Fakhfakh, S., Baklouti, S., Baklouti, S., Bouaziz, J., Elaboration and characterisation of low cost ceramic support membrane, Adv. Appl. Ceram, 109, 2010, 31-38.